

Characterization of Physically Activated *Acacia mangium* Wood-Based Carbon for the Removal of Methyl Orange Dye

Mohammed Danish,^{a,b} Rokiah Hashim,^{a,*} M. N. Mohamad Ibrahim,^b and Othman Sulaiman^a

In this experiment, *Acacia mangium* wood was physically activated in the presence of CO₂ gas at an activation temperature of 500 °C for 2 h. The total surface area of the activated carbon was found to be 395.91 m²/g, 81.06% of which was due to micropores. Fourier transform infrared spectroscopy showed that the major functional groups on the surface of activated carbon were carboxylate, hydroxyl, and lactone groups. An isotherm study of methyl orange dye adsorption by the activated carbons was conducted. Langmuir, Freundlich, Temkin, and Dubinin-Radushkevich (D-R) isotherms were applied to find the adsorption characteristics of the activated carbon. The results showed that the isotherm data followed the Langmuir isotherm with maximum adsorption capacity of 7.54 mg/g at a temperature of 25 °C and an equilibrium time of 48 h. A dimensionless equilibrium constant, R_L equal to 0.3280 was also determined to prove that adsorption was favorable but not very effective.

Keywords: *Acacia mangium* wood; Adsorption; Physical activation; Microporous; Surface area

Contact information: a: Bioresource Research lab., School of Industrial Technology, Universiti Sains Malaysia, Penang 11800, Malaysia; b: Industrial Chemistry division, School of Chemical Sciences, Universiti Sains Malaysia, Penang 11800, Malaysia; *Corresponding author: hrokiah@usm.my

INTRODUCTION

Activated carbon with its high porosity and extended surface area has been used extensively in industrial purification and chemical recovery operations. It has received much attention in recent times due to its versatile application in material science. Activated carbon is the final product of an activation process of carbonaceous materials from different sources with a carbon content in the range of 70 to 90%. The activation sequence usually commences with the initial carbonization of the raw material to obtain samples with high carbon content (Daza *et al.* 1986). These qualities define an activated carbon with excellent adsorbent characteristics useful for a wide variety of processes including filtration, purification, deodorization, decoloration, and separation (Bansal *et al.* 1988). The physical properties and the chemical composition of the precursor, as well as the methods and process conditions employed for activation, determine the final pore size distribution and the adsorption properties of the activated carbon (Bota *et al.* 1997).

Generally, two processes of activation of biomass have been practiced: physical activation and chemical activation (Tsyganova 2013). Physical activation is a two-step process; the first step is carbonization of raw material, then activation of the charred

material in the presence of N₂, CO₂, or steam at high temperature (Moreno-Piraján and Giraldo 2010). Physical activation does not involve any chemicals, thus reducing the cost of production.

Acacia mangium wood grows widely in tropical regions (Lange and Hashim 2001). It is an easily available raw material in Malaysia. The physically activated carbon from *Acacia mangium* wood in the presence of N₂ gas was prepared and reported for its adsorption study against Cr(VI) elsewhere (Danish *et al.* 2012). Basic properties of the wood carbonized in the presence of nitrogen gas is reported by Treusch *et al.* (2004).

The removal of color from wastewater has become environmentally important. The most widely used methods for removing color effluents from water include chemical precipitation, ion-exchange, osmosis, ozonation, solvent extraction, adsorption, and membrane filtration, *etc.*, but only that of adsorption is considered a cost-effective and easy-to-handle technique. Activated carbon has been a widely used adsorbent for dye removal from wastewater. Using activated carbon of different biomasses for dye removal from wastewater has been reported by many authors (Malik 2004; Phan *et al.* 2006; Prakashkumar *et al.* 2005; Malarvizhi and Ho 2010; Hameed *et al.* 2007; Garg *et al.* 2004). Methyl orange was selected for this adsorption study due to its widespread use in the dyeing industries. Methyl orange in aqueous solutions is found in the form of ionic micelles with an average molecular size of 26.14 Å.

The aim of this research was to characterize the physical and chemical nature of physically activated *Acacia mangium* wood carbon and determine its application for methyl orange dye removal. The removal isotherm data were applied to various isotherm models to determine the actual mechanism of adsorption.

EXPERIMENTAL

Preparation of Granular Activated Carbon (GAC) from *Acacia mangium* Wood

A dried wood log of *Acacia mangium* was cut into small pieces and dried in an oven at 105 °C for 12 h. The dried pieces were ground into a powder and were sieved to a particle size between 500 to 1000 µm for uniform activation. About 30 g of the material were incubated inside a muffle furnace made up of Nabertherm® equipped with temperature and time program controllers, as shown in Fig. 1, for carbonization at 350 °C for 20 min then activation at 500 °C for 120 min under a CO₂ environment. The CO₂ inlet flow rate was fixed at 200 mL/min. Almost uniform particles of granular activated carbons (GAC) were washed with an excess of demineralized water to remove any by-products formed during activation on the surface of granular activated carbon. They were dried again in an oven at 105 °C for 12 h. Dried activated carbon was kept inside sealed glass bottles for further analysis.

Characterization of *Acacia mangium* Wood Activated Carbon

Morphological and elemental composition studies using FESEM and EDX

A morphological and elemental composition study of the carbon fibers was done with a Leo Supra 50 VP Field Emission Scanning Electron Microscope (Carl-Zeiss SMT,

Oberkochen, Germany), and hyphenated with an Oxford INCA 400 energy dispersive X-ray microanalysis system (Oxford Instruments Analytical, Bucks, U.K.). This instrument can analyze SEM images and EDX with the same sample. A thin layer of gold was sputter-coated on the samples for charge dissipation during imaging.

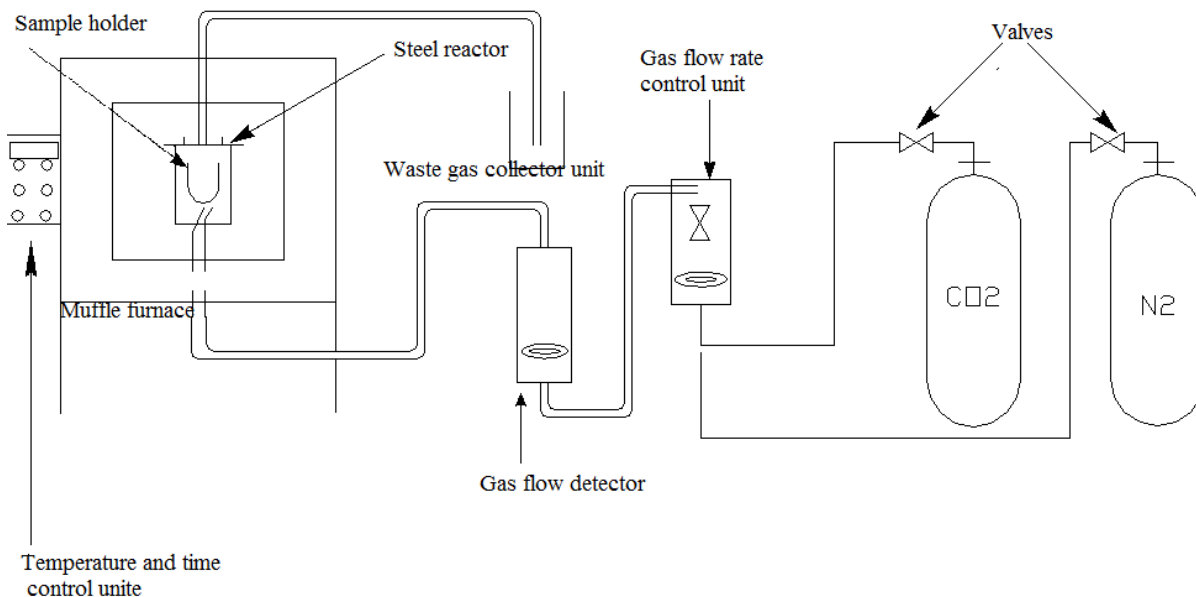


Fig. 1. Schematic diagram of carbonization and activation equipment

Fourier transforms infrared (FTIR) spectroscopy study

The FTIR spectra of the samples were recorded with a FTIR spectrophotometer (Nicolet AVATAR 380 FT-IR model), using the potassium bromide (KBr) pellet method. Oven-dried solid samples of activated carbon fiber were thoroughly mixed with KBr in a ratio of 1:100 (weight ratio of sample to KBr). The solid mixture of adsorbent and KBr were ground to a very fine powder, and compressed at 15000 psi pressure to make a thin film disk for the spectra analysis. The spectra were recorded by 64 scan with 4 cm^{-1} resolution in the mid-infrared region. Then the mid-infrared region was divided into the “group frequency” region, $4000\text{--}1300\text{ cm}^{-1}$ ($2.50\text{--}7.69\text{ }\mu\text{m}$), and the fingerprint spectral region, $1300\text{--}650\text{ cm}^{-1}$ ($7.69\text{--}15.38\text{ }\mu\text{m}$).

X-ray diffraction (XRD) study

The powder X-ray diffraction (XRD) measurements were performed by using Cu K α radiation (40 kV, 30 mA, $\lambda = 1.54\text{ \AA}$) with a step size of 0.05° glancing angle θ and with the holding time of 1 sec at a fixed angle, θ . The 1 mm thick powder sample was placed on a plastic holder and the diffraction spectra were recorded at $25\text{ }^\circ\text{C}$ and data were analyzed using Bruker DiffracPlus computer software. The XRD analysis was carried out on powdered samples to investigate the structural changes that occur during activation.

Surface area and pore size study

A nitrogen adsorption-desorption isotherm was obtained at -196 °C using a Micromeritics® ASAP2020 surface area and pore size analyzer. The specific surface area was determined by the BET, BJH, and D-R isotherm equations, and pore size distribution was calculated with the adsorption data based on original density functional theory.

pH_{zpc} determination method

The pH_{zpc} was determined by using the acid base titration method reported by Rivera-Utrilla *et al.* (2001). The pH of aliquots of 50 mL of 0.01 M NaCl solutions in conical flasks was adjusted between 2.0 and 11.0 by the addition of a 0.01 M solution of HCl or NaOH. When constant pH was achieved for each solution, 0.15 g of activated carbon sample was added into each conical flask. The flasks were set to constantly shake for 24 h.

A blank was also prepared without activated carbon to eliminate the influence of CO₂ on pH. The pH_{zpc} value was calculated at the point of intersection of the curve pH_{final} versus pH_{initial} and the line where pH_{initial} = pH_{final}.

Percentage burn-off and yield

The characterizations of the samples were carried out at their optimal working condition. The activated carbon obtained after activation was evaluated for burn-off percentage. Burn-off is defined as the weight difference between the precursor biomass and the activated carbon, divided by the weight of the precursor biomass, with both masses on a dry weight basis (Reed and Williams 2004). The yield of the activated carbon was defined as the ratio of the weight of obtained activated carbon to that of the raw wood powder with both weights on a dry basis after removing the undesired materials.

Proton absorption capacity (Q) determination method

An amount (0.1 g) of activated carbon sample was transferred into an Erlenmeyer flask and 20 mL of a 0.1 M NaCl solution was added as a background electrolyte solution. Then 1 mL of either 0.1 M HCl or 0.1 M NaOH solution was added to change the pH of the activated carbon and 0.1 M NaCl mixture. With this initial pH, the flask was agitated at room temperature to attain equilibrium. The change in pH during attaining equilibrium was converted into proton binding capacity (Q) of the activated carbon using the following equation,

$$Q = \frac{(V_0 - V_t)}{m} ([H]_i - [OH]_i - [H]_e + [OH]_e) \quad (1)$$

where V_0 and V_t are the volumes of background electrolyte (0.1 M NaCl) and the titrant (0.1 M NaOH or 0.1 M HCl) added, and m is the mass of adsorbent. Substituents i and e refer to initial and equilibrium concentrations, respectively.

Stock solution

The stock solution of methyl orange dye (1000 mg/L) was prepared by dissolving $C_{14}H_{14}N_3NaO_3S$ (mol. wt., 327.34 g/mol) (Sigma-Aldrich chemicals) in double-distilled water. The solution was further diluted to the required concentration before use.

Adsorption study

All adsorption isotherm experiments were carried out by shaking 40 mg of adsorbent with 25 mL of adsorbate solution of concentrations of 50, 75, 100, 125, 150, 200, and 300 ppm in 250 mL conical flasks. The flasks containing dye solution and activated carbon were placed on an orbital shaker for 48 h at the required temperature and fixed agitation speed of 100 rpm. The equilibrium concentrations were measured with a UV-VIS spectrophotometer. The uncertainty in temperature was $T \pm 0.5^\circ\text{C}$. All the measurements were carried out in triplicate to avoid a discrepancy in experimental results.

For generation of adsorption isotherm data, experiments were conducted at the unadjusted pH of the methyl orange dye (pH 6.3) and all the operations were performed at room temperature (25°C). The calculation of isotherm parameters and their corresponding coefficient of determination, R^2 , and hybrid fractional error (HFE) were performed.

Hybrid fractional error (HFE)

Hybrid fractional error (HFE) (Kundu and Gupta 2006) was employed to help determine which model best represented the adsorption isotherm between methyl orange and *Acacia mangium* wood-based activated carbon. This error function is more reliable than the co-efficient of regression and other error functions. It compensates for low concentrations by balancing absolute deviation against functional error (Porter *et al.* 1999). Eq. 2 was used to calculate hybrid functional error (HFE),

$$HFE = \frac{100}{(N - P)} \sum_1^N \left[\frac{|(q_{e,exp} - q_{e,cal})|}{q_{e,exp}} \right]_i \quad (2)$$

where N represents the number of data points and P is the number of parameters in the isotherm model. The $q_{e,exp}$ is the adsorption capacity at equilibrium determined experimentally, and $q_{e,cal}$ is the adsorption capacity at equilibrium determined according to the model.

RESULTS AND DISCUSSION**Surface Characterization of Granular Activated Carbon**

The field emission scanning electron microscopy (FESEM) image shown in Fig. 2 compares the changes in surface morphology before and after activation. It can be seen from the images that raw wood has a plain surface with no pore openings, whereas after activation the surface became rough with widely-scattered pores. This pore formation

with an irregular surface is suitable for the adsorption processes. The surface composition of elements determined through EDX showed that the raw wood had 51.75% carbon and 48.25% oxygen, whereas after activation the carbon percentage rose to 84.37% and the oxygen percentage was reduced to 15.63%. The reduction in oxygen percentage and increase in carbon percentage at the surface of activated carbon is due to the removal of less stable volatile matters in the form of fumes, mostly composed of oxygen derivatives from the wood surface during the carbonization and activation processes.

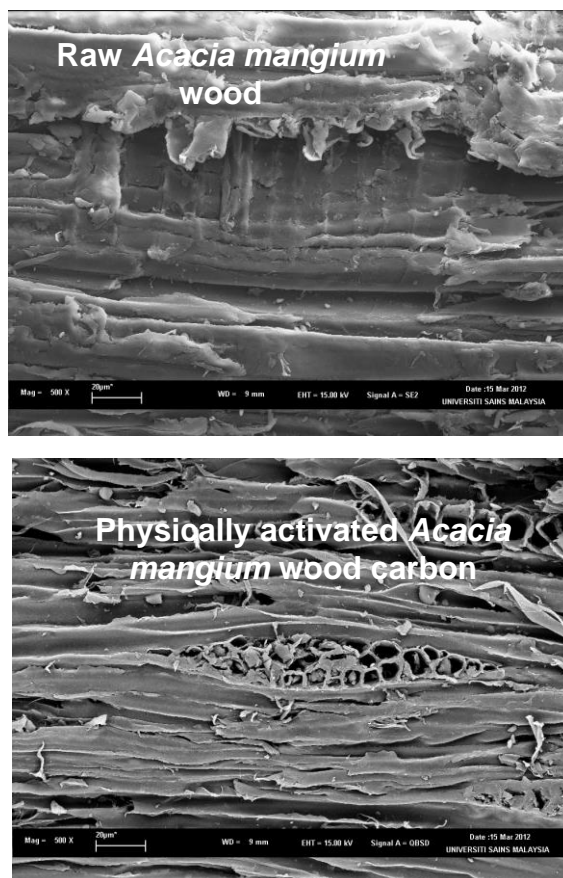


Fig. 2. Field emission scanning electron microscope images of samples

Fourier transform infrared spectroscopy spectrum is shown in Fig. 3(a) and 3(b) for raw *A. mangium* wood and physically activated carbon of *A. mangium* wood, respectively. A comparative study of the two spectra showed more peaks in the raw wood spectrum than activated carbon from the same wood. The number of peaks directly indicates the presence of functional groups, hence, raw wood has more functional groups than the activated carbon form of the raw wood. The loss of functional groups is due to heat treatment during activation. Raw wood has a broad peak at 3409 cm^{-1} that may be due to the stretching frequency of -OH groups; in activated carbon this peak shifted to 3378 cm^{-1} with diminished peak broadness. A major sharp peak in activated carbon occurred at 1587 cm^{-1} and a complementary peak at 1431 cm^{-1} indicated the presence of carboxylate functional groups at the surface. Another peak at 1692 cm^{-1} and its

complementary peak at 1236 cm^{-1} in activated carbon were probably due to lactones. The presence of a transmittance peak at 877 cm^{-1} and 756 cm^{-1} in activated carbon were due to out-of-plane aromatic C-H deformation vibration containing isolated hydrogen and an out-of-plane aromatic C-H deformation vibration containing four adjacent hydrogen atoms (Coates 2000).

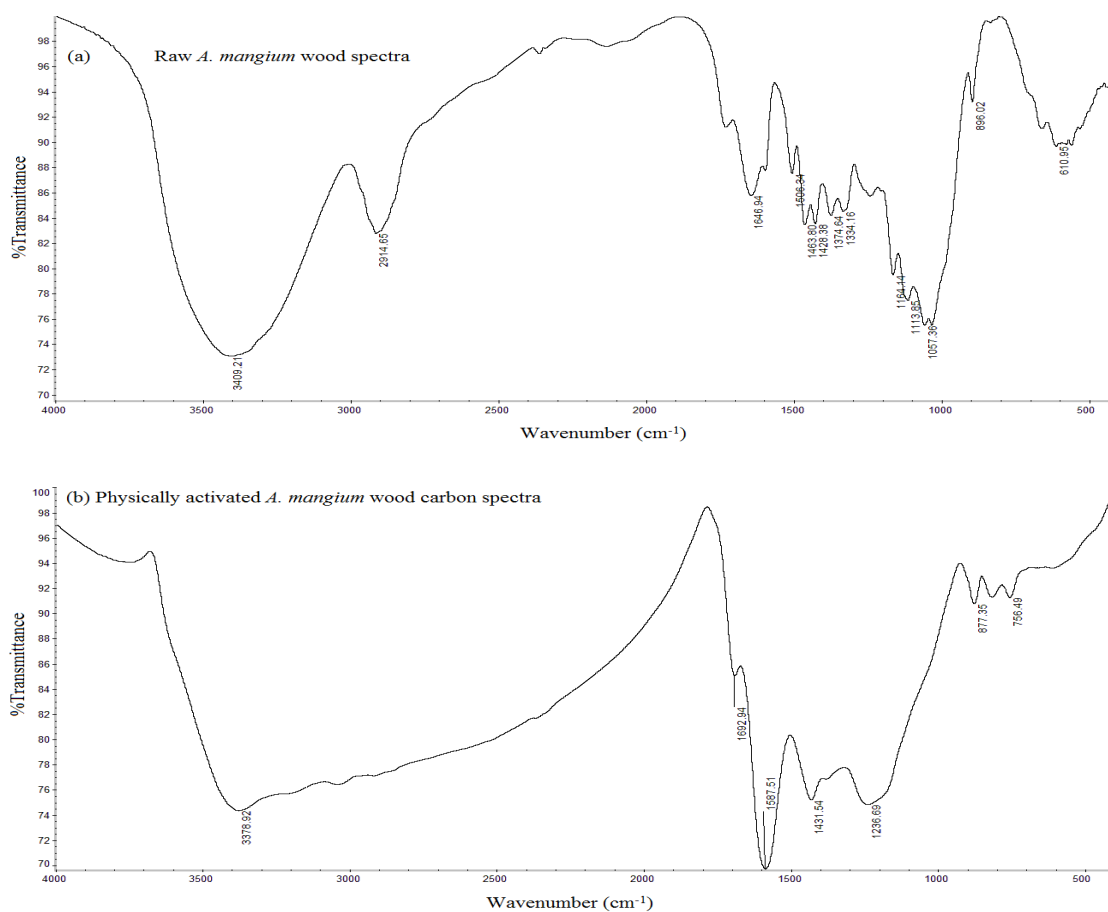


Fig. 3. FTIR spectra of (a) raw and (b) activated carbon of *Acacia mangium* wood

A powder x-ray diffraction spectrum of physically activated *A. mangium* wood carbon is shown in Fig. 4. The reflection pattern of the spectrum resembled an amorphous solid material, with the only peak at $2\theta=29.25^\circ$ indicating the presence of some microcrystalline geometry of assembled atoms in the activated carbon. The interlayer distance of the microcrystal lattice was calculated to be around 3.05 \AA and miller indices, (h,k,l) were $(1,2,10)$.

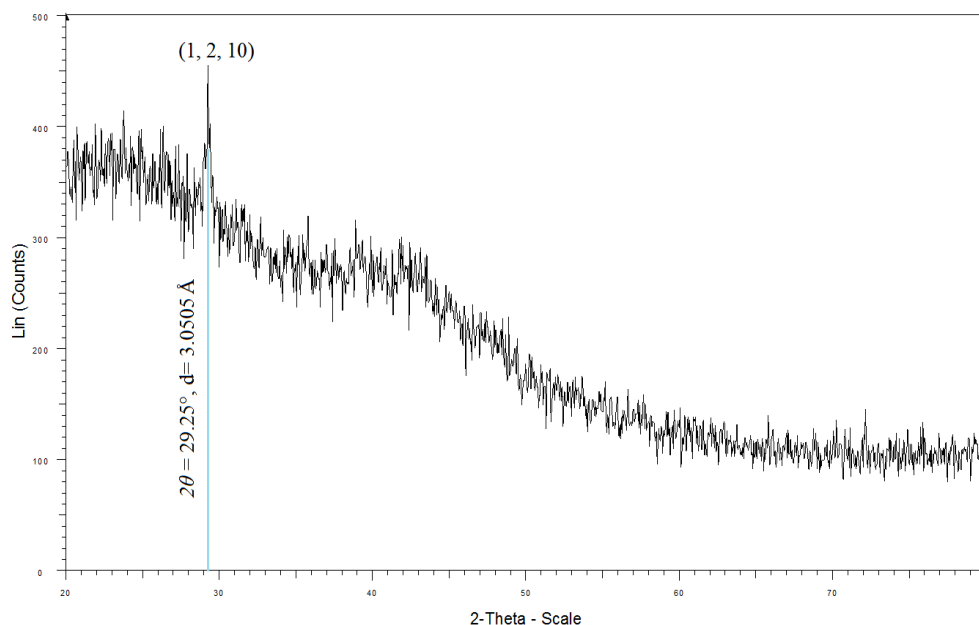


Fig. 4. XRD reflection pattern of physically activated carbon of *A. mangium* wood

The adsorption-desorption isotherm of N_2 at -195.83 °C was investigated to determine the surface area and pore texture of prepared activated carbon. According to International Union of Pure and Applied Chemistry (IUPAC) nomenclature, all the adsorption-desorption curves lie within four types of hysteresis model plots or six types of physisorption isotherm curves (Sing *et al.* 1984). For this study, it was found that the obtained adsorption-desorption curve had a hysteresis of the H4 type and the physisorption isotherm was a mixture of type I and type II curves. The initial part of the adsorption isotherm indicated a micropore filling, while the plateau of the curve parallel to the x-axis indicated a monolayer adsorption on the surface. The very small curvature at the top end is referred to as multilayer adsorption on the external surface. The adsorption-desorption isotherm of the activated carbon formed a hysteresis loop, which is characteristic of ink-bottle shaped types of pores.

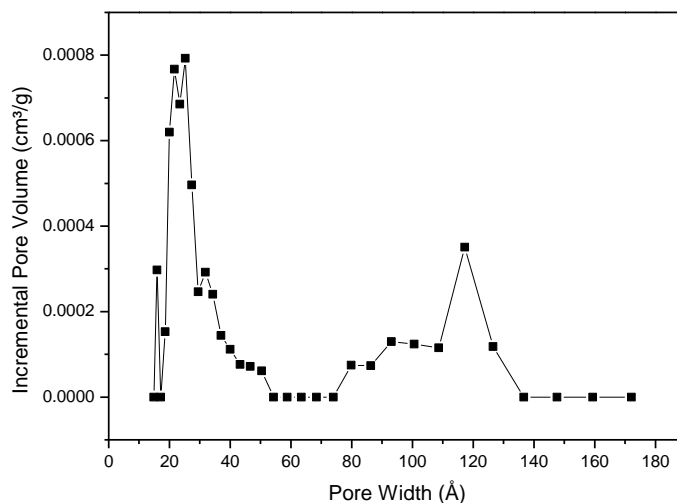
Table 1 represents the textural parameters of activated carbon deduced from N_2 adsorption isotherms. It was found that 81.06% of the total area was in the micropore area and the total external surface area was found to be 78.71 m^2/g . The micropore volume was found to be 72.68% of the total single point adsorption volume.

Table 1. Physical Characteristics and Surface Properties of Physically Activated *Acacia mangium* Wood Carbon

| S.N. | Parameters | Units | <i>Acacia mangium</i> wood activated carbon |
|------|----------------------------|--------------------|---|
| 1. | BET surface area | m ² /g | 395.9 |
| 2. | Langmuir surface area | m ² /g | 465.6 |
| 3. | Micropore surface area | m ² /g | 317.2 |
| 4. | Pore volume | cm ³ /g | 0.176 |
| 5. | Micropore vol | cm ³ /g | 0.126 |
| 5. | Av. Pore dia. | nm | 1.77 |
| 6. | pH _{zpc} | - | 6.16 |
| 7. | Burn-off | % | 70.56 |
| 8. | Yield | % | 29.45 |
| 9. | Proton absorption capacity | mmol/g | 0.000403 |
| 10. | Carbon | % | 84.37 |
| 11. | Oxygen | % | 15.63 |

Figure 5 shows the pore size distribution calculated by the means of the original density functional theory by N₂ adsorption data. The maximum incremental surface area and pore volume were observed at a pore width of 20.43 Å (micropore range of pore width). From this result it was deduced that the obtained activated carbon is composed of mostly micropores.

The pH_{zpc} was found to be 6.16, which indicated that the surface of the activated carbon was nearly neutral. The proton-binding isotherm of the physically activated carbon from *A. mangium* wood at different pH values is reported in Fig. 6. When the isotherm lies in the positive regions of the *Q* values, it signifies that protons associate with the surface at that pH range. After pH 6 the isotherm was found in the negative regions of the *Q* values, which indicated the dissociation of protons in that pH range (Puziy *et al.* 2002).

**Fig. 5.** Pore size distribution plot for physical activated *Acacia mangium* wood carbon

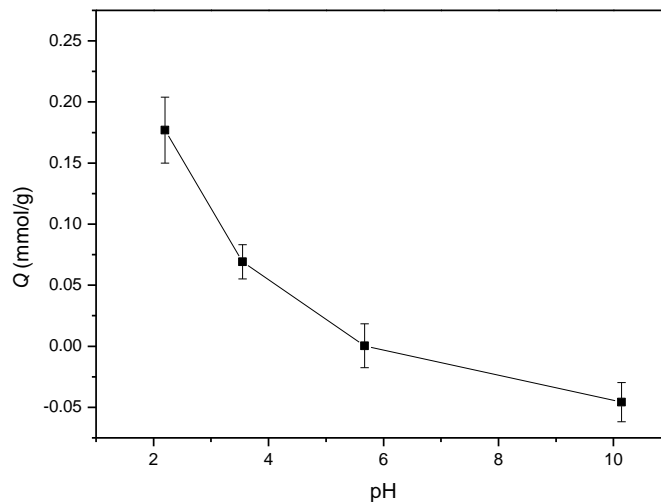


Fig. 6. Proton absorption capacities (Q) of *A. mangium* wood activated carbon at different pH values

Adsorption Isotherm Study of Methyl Orange Dye

The adsorption isotherm is a fundamental approach and plays a significant role in the determination of the maximum adsorption capacity of the adsorbent. It also provides clear and concise information about the migration of adsorbate molecules on the activated carbon surface in terms of arrangement (monolayer or multilayer), energy involved in adsorption, and rate of migration (Tsai *et al.* 2005). This will help in discovering how efficiently activated carbon will adsorb and allows for an estimation of the economic viability of the produced activated carbon. Additionally, the adsorption equilibrium data of methyl orange dye onto physically activated carbon of *Acacia mangium* wood was evaluated through the Langmuir, Freundlich, Temkin, and Dubinin-Radushkevich isotherm models.

Langmuir isotherm

The original theory of Langmuir isotherm model (Langmuir 1916) was proposed to describe the adsorption mechanism of gas molecules onto metal surfaces. Later, the same isotherm with some change in terminology has been successfully applied to many liquid to solid phase adsorption studies. The linearized Langmuir model is represented in equation below (Eq. 3).

$$\frac{1}{q_e} = \frac{1}{q_m} + \left(\frac{1}{q_m K_L}\right) \frac{1}{[C_e]} \quad (3)$$

where q_e is the equilibrium adsorption capacity (mg/g), q_m is the maximum adsorption capacity based on model C_e -equilibrium adsorbate concentration (mg/L), and K_L is the Langmuir constant. According to the Langmuir model isotherm plot, it is suggested that experimental data points were linearly fitted to the Langmuir model. The co-efficient of

regression was found to be 0.9749 and the hybrid fractional error was calculated to be 6.677. The Langmuir constants and maximum adsorption capacities values projected through the model are given in Table 2. It can be seen that a Langmuir isotherm provided the best fit with the lowest value for HFE.

Freundlich Isotherm model

To check the multilayer adsorption characteristics of methyl orange onto physically activated *Acacia mangium* wood carbon, the obtained adsorption isotherm data were applied to the Freundlich isotherm model (Freundlich 1906). The mathematical form of adsorption isotherm model is generally expressed as in Eq. 4,

$$\ln(q_e) = \ln K_f + \frac{1}{n} \ln([C_e]) \quad (4)$$

where C_e is the equilibrium adsorbate concentration (mg/L), q_e is the equilibrium adsorption capacity (mg/g), K_f (L/g), and ' n ' are Freundlich isotherm constants. The K_f represents the degree of adsorption and ' n ' represents the intensity of adsorption, where a higher value of ' n ' corresponds to a higher multilayer adsorption. The plot of $\ln(q_e)$ vs $\ln(C_e)$, was interpreted as a linear curve with a co-efficient of regression 0.9624 and a HFE as 8.2401 (given in Table 2). It was observed that the experimental data points deviated from linearity. This inferred that the model did not perfectly follow the multilayer adsorption pattern on the activated carbon surface.

D-R isotherm model

To estimate the mean adsorption energy during adsorption of methyl orange onto physically activated *Acacia mangium* wood carbon, the adsorption isotherm data were applied to the D-R isotherm (Dubinin and Raduskevich 1947). The linear form of D-R isotherm can be expressed as given in Eq.5,

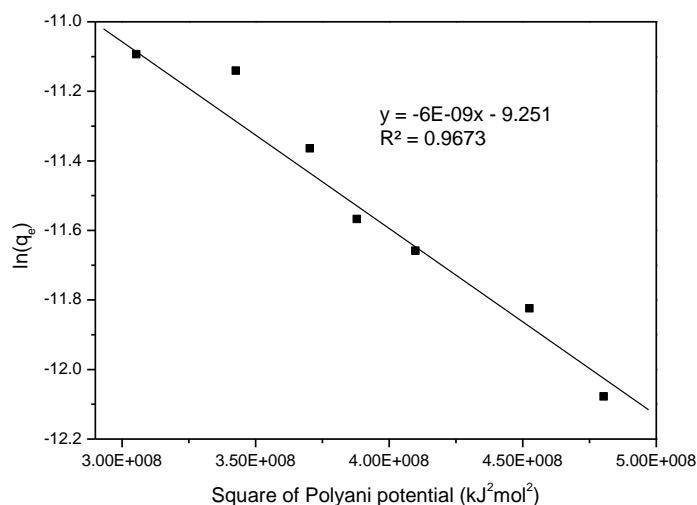
$$\ln q_{emol} = \ln q_{nmol} - \beta \varepsilon^2 \quad (5)$$

where ε represents the Polanyi potential, q_{emol} is the equilibrium adsorption capacity (mol/g), and q_{nmol} is the maximum adsorption capacity based on the D-R model (mol/g). β is constant and is determined by the slope of the $\ln q_{emol}$ vs ε^2 plot as shown in Fig. 7 and is related to mean adsorption energy, E (kJ/mol) by the following relation (Eq. 6).

$$E = \frac{1}{\sqrt{2\beta}} \quad (6)$$

Table 2. Adsorption Isotherm Parameters of Methyl Orange Removal by *Acacia mangium* Wood Activated Carbon

| Langmuir isotherm constants | Values |
|--|--------|
| q_m (mg/g) | 7.547 |
| b (L/mg) | 0.007 |
| R_L | 0.3280 |
| R^2 | 0.9749 |
| HFE | 6.6777 |
| Freundlich isotherm constants | |
| K_F (mg/g) | 0.220 |
| $1/n$ | 0.5672 |
| R^2 | 0.9624 |
| HFE | 8.2401 |
| Dubinin–Radushkevich isotherm constants | |
| $\beta \times 10^{-8}$ (mol ² /J ²) | 0.600 |
| q_m (mg/g) | 0.031 |
| E (kJ/mol) | 9.128 |
| R^2 | 0.9673 |
| HFE | 10.293 |
| Tempkin isotherm constants | |
| B_T | 1.8458 |
| K_T (mg/L) | 0.0556 |
| R^2 | 0.9548 |
| HFE | 7.8979 |

**Fig. 7.** D-R isotherm plot for adsorption of methyl orange onto physically activated carbon of *Acacia mangium* wood

With the help of the mean adsorption energy, the physical and chemical nature of the adsorption can be predicted. The values of E , in the range of 8–16 kJ/mol points towards the chemical ion exchange nature of adsorption. If the value of E is less than 8 kJ/mol, it predicts the physical nature of the adsorption process. Methyl orange adsorption onto physically activated *Acacia mangium* wood carbon gave a mean energy of adsorption of $E=9.128$ kJ/mol (given in Table 2), which lies in the chemical ion-exchange range. From the D-R isotherm results it can be interpreted that the mechanism of adsorption was not physical in nature, but rather due to a chemical interaction between the surface of the activated carbon and methyl orange. The probable interaction between the activated carbon surface and methyl orange is given in Fig. 8. The pH of the methyl orange solution was found to be 6.27, which is above the pH_{ZPC} of the activated carbon, hence, it was expected that H^+ ions were released from the surface of the activated carbon into the solution. The presence of H^+ ions in the solution induces a positive charge on the terminal nitrogen of the methyl orange (Pires *et al.* 2012), and the positively charged terminal group in methyl orange helps in adsorption through an ion-exchange mechanism.

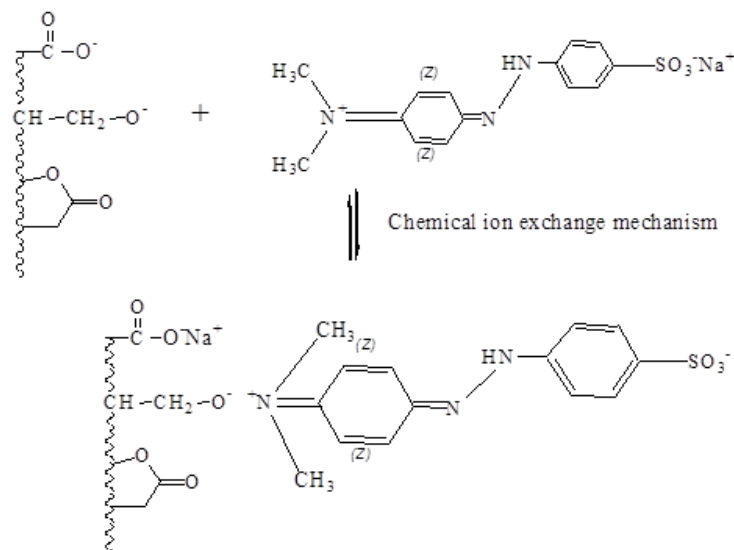


Fig. 8. Adsorption mechanism of methyl orange onto *Acacia mangium* wood activated carbon.

Temkin isotherm model

To determine the heat of adsorption and the adsorbate-adsorbate interaction in adsorption of methyl orange onto physically activated *Acacia mangium* wood carbon, the adsorption isotherm data were applied to the Temkin isotherm. The Temkin isotherm model was the result of the studies of Temkin and Pyzhev (1940) for modification of the Langmuir model. The linearized form of the model is given in Eq. 7,

$$q_e = B_T \ln(A_T) + B_T \ln(C_e) \quad (7)$$

$$B_T = \frac{RT}{b_T} \quad (8)$$

where q_e is the equilibrium adsorption capacity (mg/g), C_e is the equilibrium adsorbate concentration (mg/L), R is the universal gas constant (8.314 J/K/mol), T is the absolute temperature, A_T is the equilibrium binding constant (L/mg), and B_T is related to the heat of adsorption. The plot of q_e vs. $\ln C_e$ gives a nearly straight-line plot; the correlation coefficient value was found to be 0.9548, which showed that the isotherm data closely followed this model. The applicability of this model supports the monolayer adsorption pattern of methyl orange onto the activated carbon surface.

Based on the applicability of the above discussed model, the model predicted adsorption capacities (q_e) for each equilibrium concentration of methyl orange (C_e) which were plotted on a graph between the C_e vs q_e as shown in Fig. 9. It was found that the experimentally observed adsorption capacity values closely followed the Langmuir lines. It can be inferred from the result that adsorption of methyl orange occurred as a monolayer at the surface of activated carbon. The activated carbon contained around 81.06% of the total surface area in micropore area (pore size $<20 \text{ \AA}$) with ink bottle shaped pores and 72.68% of the total volume consisted of micropores. The methyl orange molecules have a large molecular size ($\sim 26.14 \text{ \AA}$) in aqueous solution; hence, they can fit only into those micropores that have dimensions nearly or greater than 20 \AA .

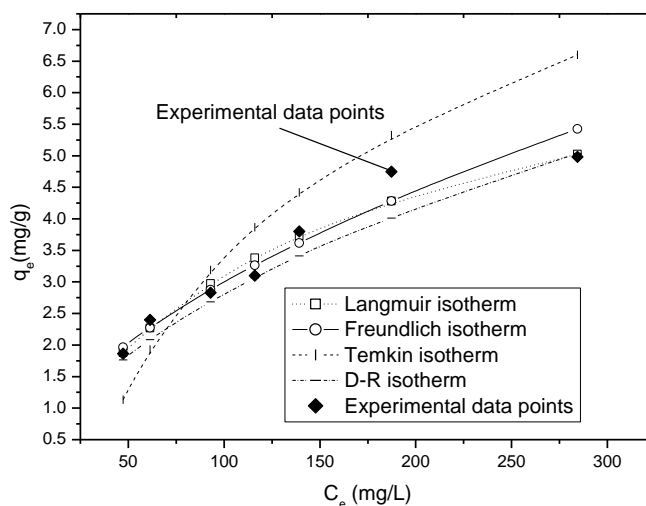


Fig. 9. Isotherm plot for methyl orange adsorption onto *Acacia mangium* wood activated carbon at 25 °C

CONCLUSIONS

1. The activation of *Acacia mangium* wood in the presence of CO_2 gas at 500 °C produced granular activated carbon with a large percentage of micropores.

2. The BET surface area of physically activated *Acacia mangium* wood carbon was found to be 395.9 m²/g.
3. The CO₂ activated *Acacia mangium* wood based activated carbon was relatively ineffective for methyl orange dye removal. It was found that the major part of the activated carbon was composed of micropores of size less than 20 Å, whereas the methyl orange dye molecules size was more than 26.14 Å in aqueous solution.
4. The maximum adsorption capacity of the *Acacia mangium* wood activated carbon was found to be 7.547 mg/g through Langmuir isotherm model.

ACKNOWLEDGMENTS

The authors acknowledge Universiti Sains Malaysia for a Post-Doctoral Fellowship to Mohammed Danish.

REFERENCES CITED

- Bansal, R. C., Donnet, J. -B., and Stoeckli, F. (1988). *Active Carbon*: Marcel Dekker Inc., New York.
- Bota, A., Laszlo, K., Nagy, L. G., and Schlimper, H. (1997). "Active carbon from apricot pits," *Magyar Kemiai Folyoirat* 103(9), 470-479.
- Coates, J. P. (2000). *A Practical Approach to the Interpretation of Infrared Spectra*, John Wiley and Sons Ltd., Chichester.
- Danish, M., Hashim, R., Ibrahim, M. N. M., Rafatullah, M., and Sulaiman, O. (2012). "Surface characterization and comparative adsorption properties of Cr(VI) on pyrolysed adsorbents of *Acacia mangium* wood and *Phoenix dactylifera* L. stone carbon," *J. Anal. Appl. Pyrol.* 97(0), 19-28.
- Daza, L., Mendioroz, S., and Pajares, J. A. (1986). "Preparation of Rh/active carbon catalysts by adsorption in organic media," *Carbon* 24(1), 33-41.
- Dubin, M. M., and Raduskevich, L. V. (1947). "The equation of the characteristic curve of the activated charcoal," *Proceedings of World Academy of Science USSR Phys. Chem. Sect.* 55(0), 331-337.
- Freundlich, H. M. F. (1906). "Over the adsorption in solution," *J. Phys. Chem.* 57, 385-471.
- Garg, V. K., Kumar, R., and Gupta, R. (2004). "Removal of malachite green dye from aqueous solution by adsorption using agro-industry waste: A case study of *Prosopis cineraria*," *Dyes Pigments* 62(1), 1-10.
- Hameed, B. H., Ahmad, A. A., and Aziz, N. (2007). "Isotherms, kinetics and thermodynamics of acid dye adsorption on activated palm ash," *Chem. Eng. J.* 133(1-3), 195-203.
- Kundu, S., and Gupta, A. K. (2006). "Arsenic adsorption onto iron oxide-coated cement (IOCC): Regression analysis of equilibrium data with several isotherm models and their optimization," *Chem. Eng. J.* 122(1-2), 93-106.

- Lange, W., and Hashim, R. (2001). "The composition of the extractives from unaffected and heartrot affected heartwood of *Acacia mangium* Willd.," *Eur. J. Wood Wood Prod.* 59(1), 61-66.
- Langmuir, I. (1916). "The constitution and fundamental properties of solids and liquids," *J. Am. Chem. Soc.* 38(0), 2221-2295.
- Malarvizhi, R., and Ho, Y. -S. (2010). "The influence of pH and the structure of the dye molecules on adsorption isotherm modeling using activated carbon," *Desalination* 264(1-2), 97-101.
- Malik, P. K. (2004). "Dye removal from wastewater using activated carbon developed from sawdust: adsorption equilibrium and kinetics," *J. Hazard. Mater.* 113(1-3), 81-88.
- Moreno-Piraján, J. C., and Giraldo, L. (2010). "Study of activated carbons by pyrolysis of cassava peel in the presence of chloride zinc," *J. Anal. Appl. Pyrol.* 87(2), 288-290.
- Phan, N. H., Rio, S., Faur, C., Le Coq, L., Le Cloirec, P., and Nguyen, T. H. (2006). "Production of fibrous activated carbons from natural cellulose (jute, coconut) fibers for water treatment applications," *Carbon* 44(12), 2569-2577.
- Pires, M. J. R. G. R., Ferra, M. I. A., Marques, A. M. M. (2012). "Ionization of methyl orange in aqueous sodium chloride solutions," *J. Chem. Thermodyn.* 53(0), 93-99.
- Porter, J. F., McKay, G., and Choy, K. H. (1999). "The prediction of sorption from a binary mixture of acidic dyes using single- and mixed-isotherm variants of the ideal adsorbed solute theory," *Chem. Eng. Sci.* 54(24), 5863-5885.
- PrakashKumar, B. G., Miranda, L. R., and Velan, M. (2005). "Adsorption of Bismark Brown dye on activated carbons prepared from rubberwood sawdust (*Hevea brasiliensis*) using different activation methods," *J. Hazard. Mater.* 126(1-3), 63-70.
- Puziy, A. M., Poddubnaya, O. I., Martínez-Alonso, A., Suárez-García, F., and Tascón, J. M. D. (2002). "Synthetic carbons activated with phosphoric acid: I. Surface chemistry and ion binding properties," *Carbon* 40(9), 1493-1505.
- Reed, A. R., and Williams, P. T. (2004). "Thermal processing of biomass natural fibre wastes by pyrolysis," *International Journal of Energy Research* 28(2), 131-145.
- Rivera-Utrilla, J., Bautista-Toledo, I., Ferro-García, M. A., and Moreno-Castilla, C. (2001). "Activated carbon surface modifications by adsorption of bacteria and their effect on aqueous lead adsorption," *J. Chem. Technol. Biot.* 76(12), 1209-1215.
- Sing, K. S. W., Everett, D. H., Haul, R. A. W., Moscou, L., Pierotti, R. A., Rouquerol, J., and Siemieniewska, T. (1984). "Reporting physisorption data for gas/solid systems with special reference to the determination of surface area and porosity," *Pure Appl. Chem.* 57(4), 603-619.
- Temkin, M. J., and Pyzhev, V. (1940). "Recent modification to Langmuir isotherms," *Acta Physicochim URSS* 12, 217-225.
- Tsai, W. T., Hsien, K. J., Chang, Y. M., and Lo, C. C. (2005). "Removal of herbicide paraquat from an aqueous solution by adsorption onto spent and treated diatomaceous earth," *Bioresour. Technol.* 96(6), 657-663.

- Treusch, O., Hofenauer, A., Tröger, F., Fromm, J., and Wegener, G. (2004). “Basic properties of specific wood-based materials carbonised in a nitrogen atmosphere,” *Wood Sci. Technol.* 38(5), 323-333.
- Tsyganova, S. (2013). “Thermal treatment of sawdust and coal-tar pitch mixture to produce porous carbon materials by chemical activation,” *Wood Sci. Technol.* 47(1), 77-82

Article submitted: April 7, 2013; Peer review completed: June 24, 2013; Revised version accepted: July 5, 2013; Published: July 10, 2013.